Linear, Planar, and Tubular Molecular Structures Constructed by Double Planar Tetracoordinate Carbon D_{2h} $C_2(BeH)_4$ Species via Hydrogen-Bridged —BeH_2Be— Bonds

Xue-Feng Zhao,[a] Haixia Li,[b] Cai-Xia Yuan,[a] Yan-Qin Li,[a] Yan-Bo Wu,*[a] and Zhi-Xiang Wang*[b]

This computational study identifies the rhombic D_{2h} $C_2(BeH)_4$ (**2a**) to be a species featuring double planar tetracoordinate carbons (ptCs). Aromaticity and the peripheral BeBeBeBe bonding around CC core contribute to the stabilization of the ptC structure. Although the ptC structure is not a global minimum, its high kinetic stability and its distinct feature of having a bonded C_2 core from having two separated carbon atoms in the global minimum and other low-lying minima could make the ptC structure to be preferred if the carbon source is dominated by C_2 species. The electron deficiency of the BeH group allows the ptC species to serve as building blocks to construct large/nanostructures, such as linear chains, planar sheets, and tubes, via intermolecular hydrogen-bridged bonds (HBBs). Formation of one HBB bond releases more than 30.0 kcal/mol of energy, implying the highly exothermic formation processes and the possibility to synthesize these nanosize structures. © 2015 Wiley Periodicals, Inc.

DOI: 10.1002/jcc.24018

Introduction

Planar tetracoordinate carbon (ptC) is a peculiar bonding motif featuring a carbon encompassed by four ligands in a plane. Since the pioneering studies, including the Monkhorst's 1968 proposal of ptC transition state for the steromutation of asymmetric carbon,[1] the Hoffmann et al. 1970 EHMO analysis of planar methane,[2] and the computational prediction of the first ptC molecule (C_{2v} $C_3H_4Li_2$) by Schleyer and coworkers in 1976,[3] the field has progressed considerably.[4–9] Various ptC species or molecules have been realized experimentally or designed computationally. Furthermore, the concept of ptC bonding has also been extended to planar hypercoordinate carbon (phC)[10–16] and planar bonding arrangements of heteroatoms and transition metals.[17–26]

In addition to finding small species or molecules featuring phC(s), chemists have also explored whether the phC bonding could be applied to construct large molecular structures or bulky solids. Surveying previous studies, the reported large molecular structures/solids can be classified into three classes as summarized below.

The first class is the salt-like extendable three-dimensional solids consisting of anionic ptC units, counterions, and auxiliary ligands in some cases. Solids only containing anionic ptC units and counterions include that constructed using ptC CAl_4^{2-} and sodium as counterions and that using ptC C_5^{2-} and zinc or lithium as counterions, respectively.[27–30] Anionic cyclopentadiene ligand as the auxiliary protection group was used to design structures on the basis of ptC units such as CAl_4^{2-}, CAl_4^-, CAl_3Si, CAl_3Si^-, CB_6^{2-}, and CAl_2Si_2 with compatible alkali metal cations.[31–35]

The ptCs in the second class are confined in the periodic 1D- and 2D-structures. Examples include the B_2C graphene, nanoribbons, and nanotubes having ptCs or quasi-ptCs,[36] the binary global minima structures such as B_2C, B_3C, and B_5C monolayer sheets with ptCs,[37] the metal-decorated zigzag and armchair graphene nanoribbons with ptCs,[38–40] the metal-decorated SiC nanoribbons with both ptCs and planar tetracoordinate silicon (ptSis),[41] the Al_2C,[42,43] TiC[44], and Be_2C[45] monolayer sheets with ptCs, quasi-ptCs, and quasi-planar hexacoordinate carbons, respectively, and the nickel and cobalt surfaces embedded ptCs.[46] In addition to nanostructures with phCs, 1D or 2D nanostructures with planar hypercoordinate nitrogens, silicons, coppers[47–49] have also been reported.

The third class uses well-defined ptC species/molecules as building blocks to assemble large/nano-size molecular structures. Different form the first type, no counterion is needed. According to how the ptC building blocks are assembled, this class of structures can be further divided into two types. The structures of the first type are formed via condensation of ptC

[a] *Xue-Feng Zhao, Cai-Xia Yuan, Yan-Qin Li, Yan-Bo Wu*
The Key Laboratory of Materials for Energy Conversion and Storage of Shanxi Province, the Key Laboratory of Chemical Biology and Molecular Engineering of Education Ministry, Institute of Molecular Science, Shanxi University, Taiyuan 030006, People's Republic of China
E-mail: zxwang@ucas.ac.cn; E-mail*: wyb@sxu.edu.cn*
[b] *H. Li, Zhi-Xiang Wang*
College of Chemistry and Chemical Engineering, University of Chinese Academy of Sciences, Beijing 100049, People's Republic of China

In memory of Professor Paul von Ragué Schleyer.
Xue-Feng Zhao and Haixia Li Contribute equally.
Contract grant sponsor: National Natural Science Foundation of China; Contract grant numbers: 20973197, 21003086, 21273140, 21471092; Contract grant sponsor: Provincial Natural Science Foundation of Shanxi; Contract grant number: 2009021016

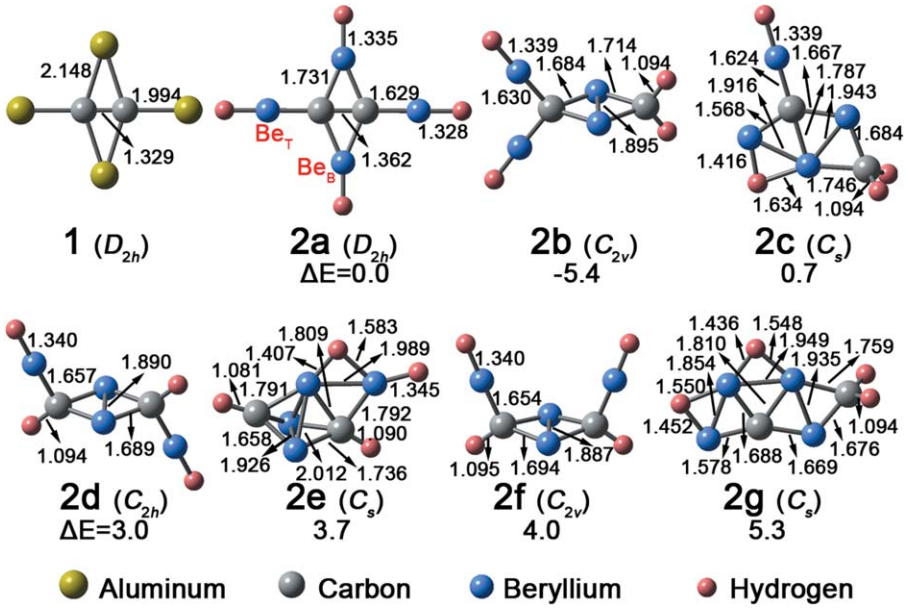

Figure 1. CCSD(T)/aug-cc-pVTZ optimized structures of C_2Al_4 and the isomers of $C_2(BeH)_4$. The bond lengths are given in Å and the relative energies (ΔE in kcal/mol) of these $C_2(BeH)_4$ isomers are based on the CCSD(T) energies corrected with B3LYP/aug-cc-pVTZ ZPE.

blocks and the interactions among blocks are covalent bonding. Examples include the belt-like, circular, and tubular molecules designed on the basis of the ptC species CM_4H_4 (M = Ni, Pd, Pt),[50] the molecular belts, rings, zigzag nanotubes, and helical nano-size molecules designed on the basis of $C_3B_2H_4$ ptC units,[51,52] and the linear, flat, and tubular molecules[53,54] using ptC species $C_2Al_4E_8$ (E = CH_3, NH_2, and OH) as the building units.[55] The structures of the second type are assemblies of ptC units, in which the integrity of the ptC units maintains. Spurred by the question whether the planarity of ptC bonding can be utilized to construct structures similar to graphene, carbon nanotubes, and fullerenes constructed by planar sp^2 carbon, we searched for ptC hexagonal building block. Interestingly, the substitutions of all hydrogen atoms of monocyclic hydrocarbons $(CH)_n^q$ ($n = 4$–9, $q = 0$, ±1, or ±2) with BeH groups led to their ptC minimum counterparts, $C_n(BeH)_n^q$ ($n = 4$–9, $q = 0$, ±1, or ±2). Among them, the so-called star-benzene (the counterpart of benzene) with six ptCs, D_{6h} $C_6(BeH)_6$, can be used to assemble molecular structures similar to graphene, fullerene, and carbon nanotubes via forming the intermolecular hydrogen-bridged -BeH_2Be- bonds (HBBs).[56] Extending this strategy, we herein report new forms of linear, planar, and tubular molecular structures assembled by double ptC units, D_{2h} $C_2(BeH)_4$ (**2a** in Fig. 1).

Methods

The potential energy surface (PES) of stoichiometric $C_2Be_4H_4$ was explored using the stochastic search algorithm.[57,58] The geometries were generated randomly and then optimized at the B3LYP/6-31G(d) level. To ensure convergent PES explorations, we run four sets of PES searches (two sets on singlet surface and two sets on triplet surface). The resultant lowest triplet structure is 29.2 kcal/mol higher than singlet **2a**, thus, the triplet isomers were not further considered at higher level. Twenty lowest singlet isomers at B3LYP/6-31G(d) level were then refined at the B3LYP/aug-cc-pVTZ level, including geometric reoptimizations and vibrational frequency analyses. The structures of 10 lowest isomers at B3LYP/aug-cc-pVTZ level were further optimized at the CCSD(T)/aug-cc-pVTZ level. The CCSD(T) energies corrected with the B3LYP/aug-cc-pVTZ zero point energies (ZPEs) were used to discuss the relative stabilities of these isomers. B3LYP/aug-cc-pVTZ calculations were performed to analyze the electronic structures of **1** and **2a**, including the canonical molecular orbitals, the charges and Wiberg bond indices via natural bond orbital (NBO) analyses,[59] and the nucleus-independent chemical shifts (NICS)[60,61] with the gauge-independent atomic orbital approach.[62] Because the energetic and geometric results of **2a** dimers at the B3LYP/6-31G(d) level are very close to those at the B3LYP/aug-cc-pVTZ level, large structures were calculated only at the B3LYP/6-31G(d) level. The ZPE-corrected B3LYP/6-31G(d) energies were used to evaluate the formation energies of assemblies. To assess the kinetic stability of **2a**, Born–Oppenheimer molecular dynamic (BOMD)[63] simulations were run at the B3LYP/6-31G(d) level with temperatures at 4, 298, and 500 K, respectively. The random structures for the PES explorations were generated by the GXYZ program,[64] the density functional theory (DFT) and MP2 calculations were performed using the GAUSSIAN 09 package[65] and the CCSD(T) calculations were performed using MolPro 2012.1 package.[66]

Results and Discussion

Design and structures of D_{2h} $C_2(BeH)_4$

We previously identified D_{2h} C_2Al_4 (**1**) to be a global minimum featuring double ptCs.[67] According to the diagonal relationship

Table 1. The NBO analysis results, which include the natural charges of C and X (X = Al or Be) (Q_C and Q_X), the total Wiberg bond indecies (WBI) of C and X (X = Al or Be) (WBI_C and WBI_X), and the Wiberg bond orders of C—C, C—Al, CC—X, and Be—H bonding (WBI_{C-C}, WBI_{C-Al}, WBI_{CC-X}, and WBI_{Be-H}).

	Q_C		WBI_C		WBI_{C-C}			Q_X		WBI_X		WBI_{CC-X}[c]		WBI_{Be-H}
1[a]	−1.39		3.11		2.09		Al_B	0.69		0.80		0.51		
							Al_T	0.70		0.72		0.50		
2a[a]	−1.05		3.31		1.87		Be_B	0.77		1.86		0.82		0.87
							Be_T	0.98		1.58		0.60		0.84
2a[b]	−1.06		3.28		1.83		Be_B	0.80		1.86		0.83		0.87
							Be_T	0.98		1.58		0.60		0.84
	Min[d]	Max[e]	Min	Max	Min	Max		Min	Max	Min	Max	Min	Max	
TT-C3[b]	−0.92	−1.09	3.30	3.42	1.83	1.84	Be_B	0.82	0.85	1.79	1.82	0.74	0.78	
							Be_T	0.65	0.98	1.58	2.22	0.60	0.79	
TTBB-C9[b]	−0.79	−1.01	3.37	3.55	1.84	1.89	Be_B	0.54	0.83	1.83	2.37	0.80	0.87	
							Be_T	0.65	1.00	1.56	2.22	0.56	0.76	
TTBB-T18[b]	−0.81	−0.87	3.50	3.56	1.86	1.89	Be_B	0.55	0.82	1.83	2.34	0.76	0.83	
							Be_T	0.66	0.67	2.19	2.21	0.72	0.75	

[a] Results at B3LYP/aug-cc-pVTZ level. [b] Results at B3LYP/6-31G(d) level. [c] WBI_{CC-X} means the sum of Wiberg bond orders between two carbon atoms and X atoms. [d] "Min" means the minimum values. [e] "Max" means the maximum values.

of aluminum with beryllium, we replaced Al atoms in **1** with valence isoelectronic BeH groups, leading to a planar structure with double ptCs, D_{2h} $C_2(BeH)_4$ (**2a** in Fig. 1) which was confirmed to be an energy minimum at both B3LYP/aug-cc-pVTZ and MP2/aug-cc-pVTZ levels with the smallest vibrational frequency of 76 and 69 cm^{-1}, respectively. The geometry of **2a** refined at CCSD(T)/aug-cc-pVTZ level, along with the key geometric parameters, are displayed in Figure 1. The two types of beryllium atoms in **2a** are termed as Be_T (terminal Be) and Be_B (bridged Be), respectively. The regular bond lengths of C—Be_B (1.731 Å), C—Be_T (1.629 Å), and C—C bonds (1.362 Å) geometrically indicate the ptC bonding nature.

The replacement does not alter the ptC bonding in quality but only in quantity. Formally, each of Al atoms in **1** provides one valence electron to bond to central CC core. Similarly, each of Be atoms in **2a** also contributes one electron to form bond with the central CC core. The difference lies in that the remaining two valence electrons of an Al atom in **1** form a lone pair, while a Be atom in **2a** uses the remaining one valence electron to form a Be—H single bond. Supportively, the Wiberg bond orders (WBI_{Be-H}) of the four Be—H bonds are all larger than 0.80 (Table 1). Nevertheless, the larger WBI_{CC-Be} (0.82/0.60) in **2a** than the WBI_{CC-Al} (0.51/0.50) in **1** indicates that the ptC bonding in **2a** is stronger than that in **1**. Because the CC core in **2a** uses more electrons to form bond with surrounding atoms than that in **1**, the C—C

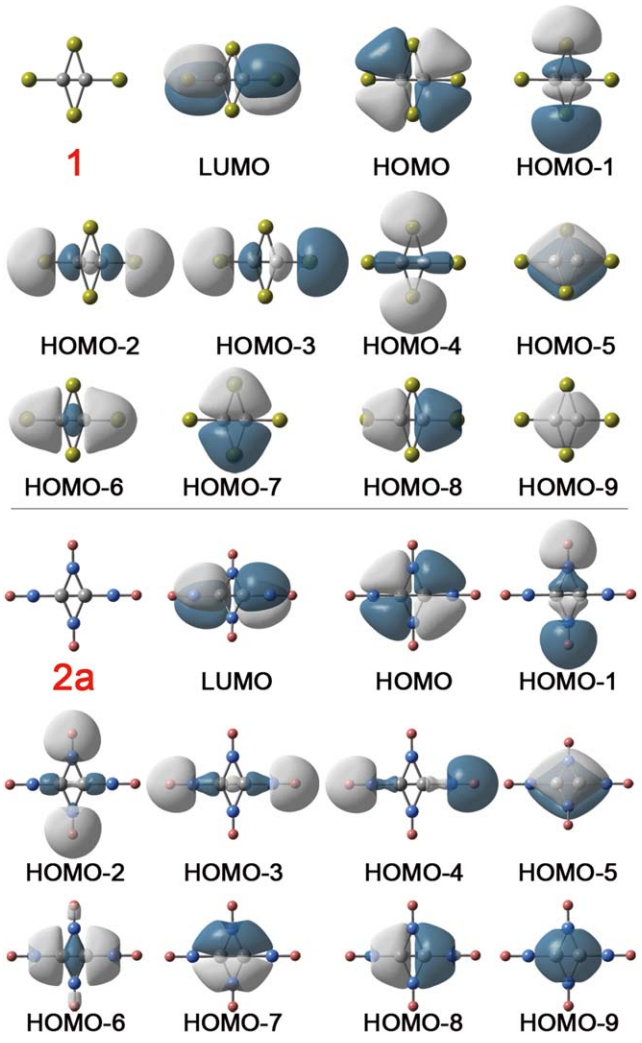

Figure 2. Comparisons of the LUMO and occupied valence MOs of **1** and **2a**.

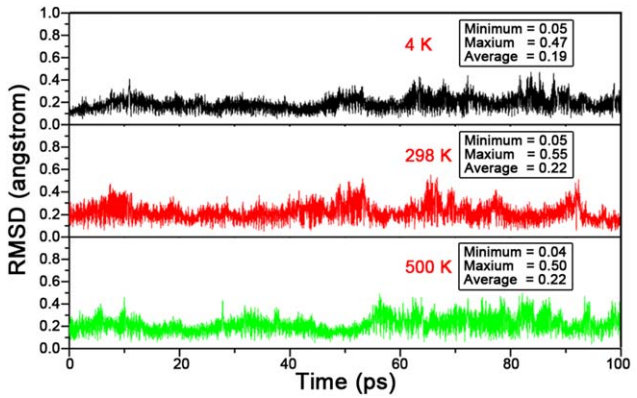

Figure 3. RMSD versus time in the BOMD simulations of **2a**. [Color figure can be viewed in the online issue, which is available at wileyonlinelibrary.com.]

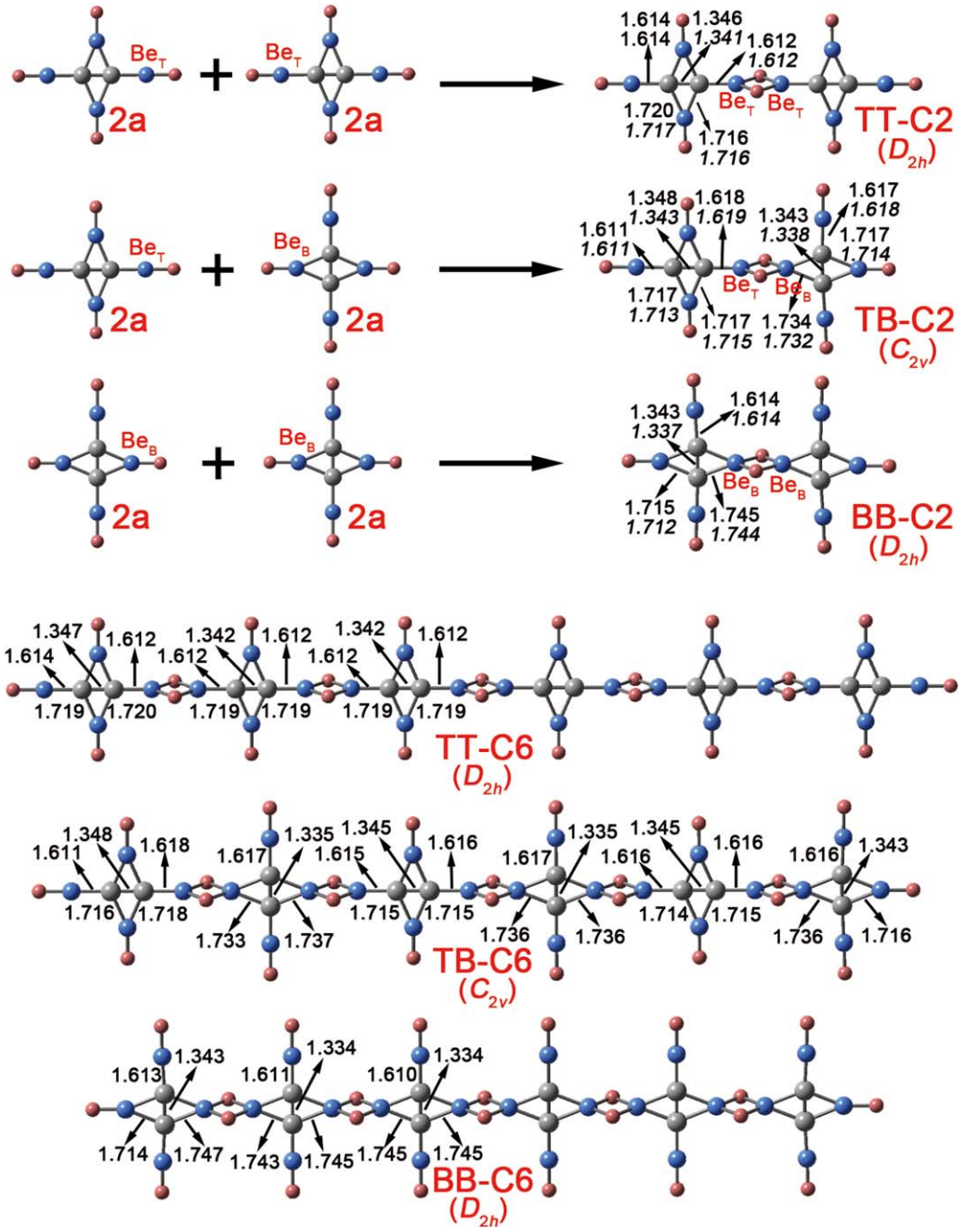

Figure 4. Optimized structures of molecular chains with key bond lengths. The bond lengths (in Å) at B3LYP/6-31G(d) and B3LYP/aug-cc-pVTZ are given in normal and italic fonts, respectively. [Color figure can be viewed in the online issue, which is available at wileyonlinelibrary.com.]

covalent bonding in **2a** is weaker than that in **1**, as reflected by the smaller WBI_{C-C} (1.87) in **2a** than in **1** (2.09) and the slightly longer C—C bond length (1.362 Å) in **2a** than that (1.329 Å) in **1**. The natural charges on C of **1** (−1.39 |*e*|) is larger than that of **2a** (−1.05 |*e*|), but the natural charges on Al atoms of **1** (+0.69/+0.70 |*e*|) are smaller than that on Be atoms of **2a** (+0.77/+0.98 |*e*|), thus, the overall contribution of electrostatic interactions between the CC core and surrounding atoms could be close in the two ptC species.

Figure 2 compares the key molecular orbitals (MOs) of **1** and **2a**. The MOs of **1** and **2a** have one-to-one correspondences except for the difference in the order of HOMO-2, HOMO-3, and HOMO-4. The four MOs (from HOMO-4 to HOMO-1) of **2a,** which describe the four Be—H bonds, are similar to those (from HOMO-4 to HOMO-1) of **1**, which describe the four lone pairs on Al atoms, indicating the equivalence of two Be—H bonding electrons in **2a** to the Al lone pair in **1**. Like **1**, **2a** also has one π orbital (HOMO-5), so it is aromatic, as verified by a negative NICS value, −15.9 ppm at the center of the C—C—Be_B triangle. The aromaticity contributes to the stabilization of ptC arrangement. In addition, the highest occupied molecular orbital (HOMO) of **2a** indicates a peripheral Be_4

Table 2. The lowest harmonic vibrational frequencies (ν_{min}, in cm^{-1}), the HOMO–LUMO gaps (Gap, in eV), the total formation energies (ΔE_{Total}, in kcal/mol), and the average formation energies per HBB (ΔE_{HBB}, in kcal/mol).[a]

	ν_{min}	Gap	ΔE_{Total}	ΔE_{HBB}
2a[b]	76	3.48		
TT-C2[b]	27	3.51	−35.8	−35.8
TB-C2[b]	28	3.10	−34.0	−34.0
BB-C2[b]	37	3.26	−30.1	−30.1
2a	92	3.51		
TT-C2	29	3.53	−35.2	−35.2
TT-C3	14	3.52	−70.1	−35.1
TT-C4	9	3.51	−105.0	−35.0
TT-C5	5	3.51	−140.0	−35.0
TT-C6	3	3.50	−174.9	−35.0
TB-C2	31	3.13	−33.8	−33.8
TB-C3_1	16	3.10	−66.8	−33.4
TB-C3_2	16	2.97	−66.8	−33.4
TB-C4	8	2.98	−100.0	−33.3
TB-C5_1	5	2.94	−133.1	−33.3
TB-C5_2	5	2.99	−133.1	−33.3
TB-C6	3	2.93	−166.2	−33.2
BB-C2	38	3.30	−30.4	−30.4
BB-C3	20	3.18	−59.9	−30.0
BB-C4	12	3.11	−89.5	−29.8
BB-C5	7	3.06	−119.0	−29.8
BB-C6	5	3.02	−148.6	−29.7
TTBB-P4	27	3.33	−130.0	−32.5
TTBB-P9	14	3.20	−385.2	−32.1
TTBB-P16	8	3.11	−766.8	−31.9
TTBB-P12	9	3.19	−547.4	−32.2
TTBB-P15	5	3.18	−709.5	−32.3
TTBB-P18	3	3.18	−871.6	−32.3
TBTB-P4	25	3.71	−135.8	−33.9
TBTB-P9	13	3.44	−401.1	−33.4
TBTB-P16	8	3.45	−799.0	−33.3
TTBB-T9	28	3.19	−304.5	−20.3
TTBB-T12	27	3.17	−514.8	−25.7
TTBB-T15	24	3.15	−704.7	−28.2
TTBB-T18	18	3.14	−884.8	−29.5

[a] At B3LYP/6-31G(d) level. [b] At B3LYP/aug-cc-pVTZ level.

bonding around central CC core. Previously, it has been shown that such a peripheral bonding around ptC plays an important role in stabilizing ptC molecules (e.g., boraplanes)[68] or species (e.g., the global minima wtih ptC D_{4h} CAl_4^{2-} and planar pentacoordinate carbon D_{5h} CAl_5^+).[27,69]

2a is an energy minimum. Next, we examined the thermodynamic stability of **2a** relative to its isomers. Figure 1 ranks the lowest seven isomers (**2a**–**2g**) according to the CCSD(T)/aug-cc-pVTZ energies corrected with the B3LYP/aug-cc-pVTZ ZPEs. The isomer **2b** featuring two tetrahedral carbons is the global minima of stoichiometric $C_2Be_4H_4$. **2a** is 5.4 kcal/mol higher than **2b** and closest to the global minimum (**2b**). Isomers **2d** and **2f** having two tetrahedral carbons are 3.0 and 4.0 kcal/mol higher than **2a**. Isomers **2c** and **2g** featuring a ptC bonding are higher than **2a** by 0.7 and 5.3 kcal/mol, respectively. The 3D isomer **2e** is 3.7 kcal/mol higher than **2a**. The isomers **2b–2d**, **2f**, and **2g** feature a rhombic C—Be_2—C bridge bonding and **2e** has a trigonal bipyramidal C—Be_3—C bridge bonding. These Be-bridged bonds could be one of factors to stabilize these structures. The two carbon atoms in **2b**–**2g** are separated, whereas **2a** uniquely maintains a bonded C_2 core. We speculate that the distinct feature could make **2a** experimentally accessible (though it is not a global minimum) if experiments can generate carbon sources dominated by C_2 species.

We further assessed the kinetic stability of **2a** by performing three sets of 100 ps BOMD simulations at B3LYP/6-31G(d) level at temperatures of 4, 298, and 500 K, respectively. As show in Figure 3, with respect to the optimized structure of **2a**, the root-mean-square deviations (RMSDs) of C_2Be_4 core are in the range of 0.05–0.47 (4 K), 0.05–0.55 (298 K), and 0.04–0.50 Å (500K), with average RMSDs of 0.18, 0.22, and 0.22 Å, respectively. The small RMSDs indicate the C_2Be_4 ptC arrangement in **2a** can be well preserved, thus, **2a** has good kinetic stability, encouraging us to use **2a** as a building block to construct large molecular structures.

Nano-size structures with $C_2(BeH)_4$ as building blocks

The ptC species D_{2h} $C_2(BeH)_4$ has four electron-deficient BeH bonds, which allows **2a** to undergo polymerization through forming intermolecular -BeH_2Be- bridge bond, resulting in large **2a** assemblies. For the convenience of description of the various assemblies, we use a string "**XX-S*n***" to term an assembly, where "**XX**" denotes the pattern of the hydrogen-bridged bonds, which could be "**TT**," "**TB**," or "**BB**" for $Be_TH_2Be_T$, Be_TH_2-Be_B, and $Be_BH_2Be_B$ bridges, respectively, "**S**" describes the shape of the assembly, which could be "**C**" for a chain, "**P**" for a planar sheet, or "**T**" for a tube, and "***n***" is the number of **2a** units that an assembly contains. For example, **TT-C2** (see Fig. 4) names a **2a** dimer formed via a $Be_TH_2Be_T$ bridge bond. At the B3LYP/6-31G(d) level, **TT-C2**, **BB-C2**, and **TB-C2** dimers are all energy minima with dimerization energies of −35.2, −30.4, and −33.8 kcal/mol, respectively. The values are close to those (−35.8, −30.1, and −34.0 kcal/mol, respectively) at the B3LYP/aug-cc-pVTZ level, thus we calculated large assemblies only at B3LYP/6-31G(d) level. The large energy released by forming the intermolecular HBBs can provide a driving force to assemble **2a** building blocks to various large structures, as shown by following examples.

Molecular chains

Similar to dimerization, **2a** can serve as building blocks to construct long linear chains via HBBs. As demonstrations, we computed three types of linear structures containing up to six **2a** units, including **TT-C3~TT-C6**, **TB-C3~TB-C6**, and **BB-C3~BB-C6**. The optimized structures with six **2a** units are displayed in Figure 4 and others are given in the Supporting Information. All these chains are energy minima at B3LYP/6-31G(d) level. The lowest vibrational frequencies of these longer chains are relatively small (ranging from 3 to 38 cm^{-1}), however, the normal modes of these vibrational frequencies do not deform the ptC arrangements but indicate the flexibility of the long molecules. Going from trimers to hexamers, the average formation energies per HBBs (ΔE_{HBB}) remains nearly the same (see Table 2).

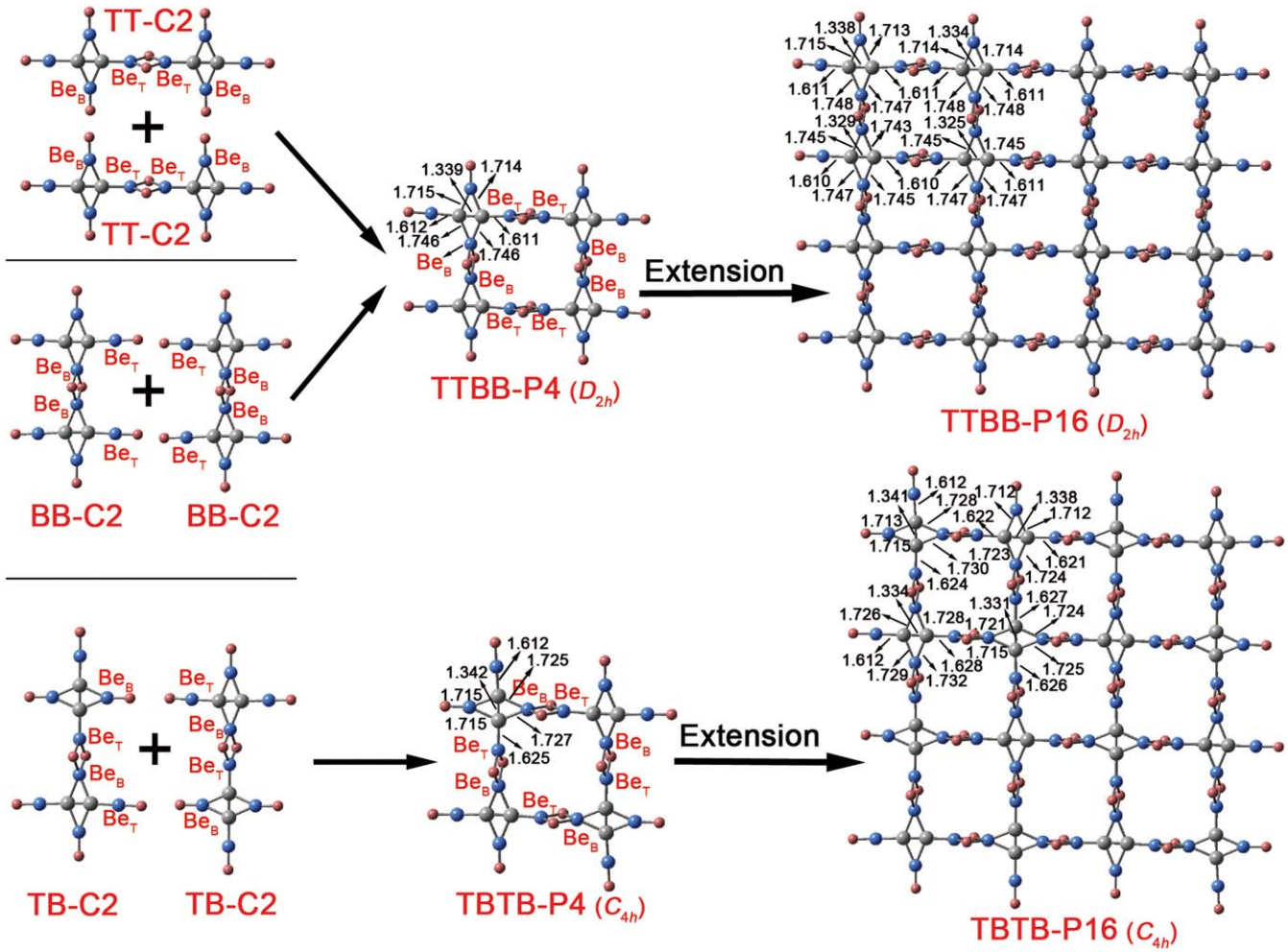

Figure 5. Construction of the planar sheets from molecular chains. The planar sheets were optimized at the B3LYP/6-31G(d) level. The key bond lengths are giving in Å. [Color figure can be viewed in the online issue, which is available at wileyonlinelibrary.com.]

Planar sheets

The chain structures only use two of its four Be-H groups of **2a**. If they are all utilized, 2D planar sheets can be formed. As illustrated in Figure 5, putting **TT**-type or **BB**-type chains side-by-side via **BB** HBBs or **TT** HBBs leads to **TTBB** planar structures. Similarly, **TB**-type chains can also be assembled into **TBTB** sheet via **TB** HBBs. As examples, we built $n \times n$ ($n = 2$–4) sheets. The optimized structures of 2 × 2 and 4 × 4 **TTBB** and **TBTB** sheets are shown in Figure 5 and that of 3 × 3 **TTBB** and **TBTB** sheet are given in the Supporting Information. Figure 6 also includes 4 × 3, 5 × 3, and 6 × 3 **TTBB** planar sheets which are built for investigating the thermodynamic stabilities of the tubular structures (see below). The average formation energies per HBBs in **TTBB-P4** and TB**TB-P4** are −32.5 and −33.9 kcal/mol, respectively. As the planar sheets are extended, the values decrease slightly to −32.1 (**TTBB-P9**) and −33.4 (**TBTB-P9**) kcal/mol and to −31.9 (**TTBB-P16**) and −33.3 (**TBTB-P16**) kcal/mol. The values for **TTBB-P18** and **TBTB-P18** are identical to that of **TTBB-P16** and **TB-P16**, respectively, indicating the extension would not decrease the thermodynamic stabilities of the large sheets.

Nanotubes

Graphene can be rolled to single-walled carbon nanotube. Similarly, the planar sheets discussed above can be rolled to the tubular structures. Unlike planar sheets, tubular structures suffer from strains and the smaller the radius of the tube is, the greater the strain is. If the strain is greater than the energy released from the formation of HBBs, the formation of tubular structures would be thermodynamically unfavorable. To find the least number of **2a** units in a layer for thermodynamically stable tubular assemblies, we constructed three-layer **TTBB** tubes with three to six **2a** units in one layer. The optimized structures of these tubes are shown in Figure 6. The 3 × 3 tube (**TTBB-T9**) is 80.7 kcal/mol higher than its planar isomer **TTBB-P9** at the B3LYP/6-31G(d) level, suggesting that the formation of the small tube is impossible. Similarly, the 4 × 3 (**TTBB-T12**) and 5 × 3 (**TTBB-T15**) tubes are still 32.6 and 4.8 kcal/mol less stable than their planar sheet isomers **TTBB-P12** and **TTBB-P15**, respectively. However, the 6 × 3 **TTBB-T18** tube is 13.2 kcal/mol more stable than its planar sheet counterpart **TTBB-P18,** indicating that a **TTBB** tube at least has six **2a** units in a layer to ensure favorable thermodynamics.

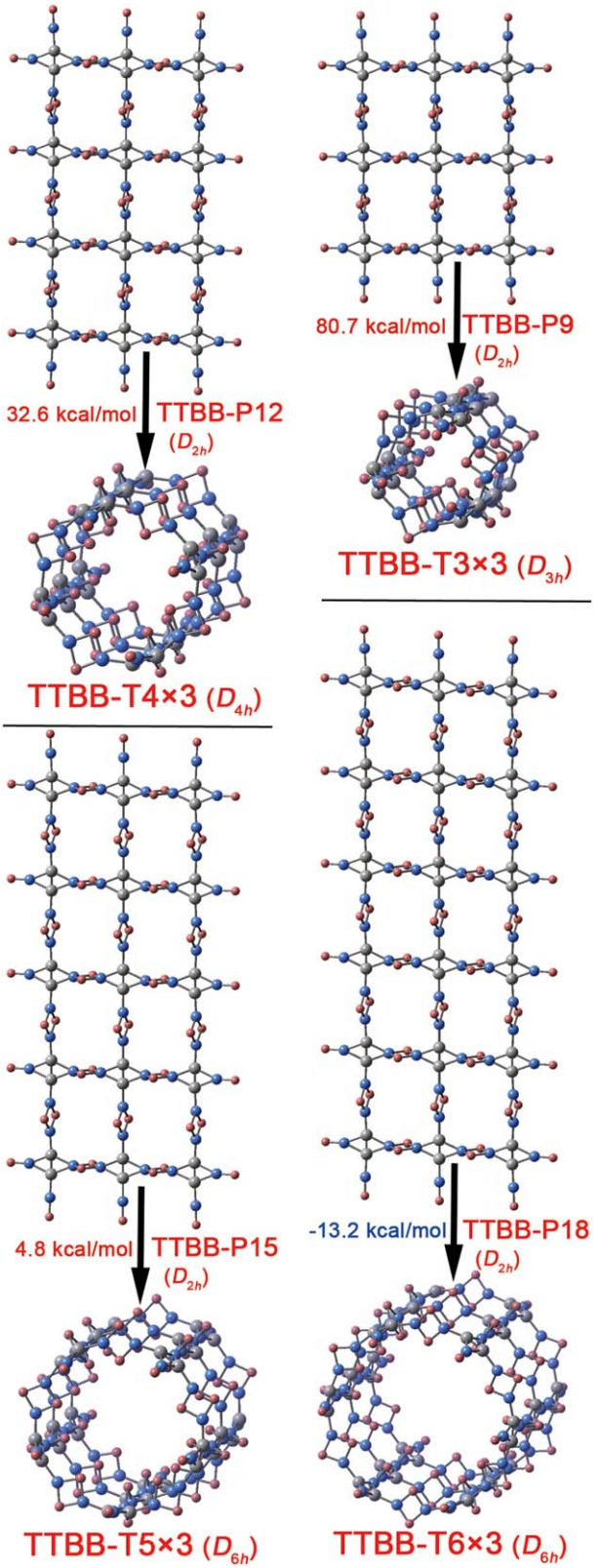

Figure 6. B3LYP/6-31G(d) optimized structures and relative energies of the nanotubes **TTBB-T*n*** (***n*** = **9**, **12**, **15**, and **18**) and their planar sheets counterparts **TTBB-P*n*** (***n*** = **9**, **12**, **15**, and **18)**. The perspective is used to view the tube structures more clearly. [Color figure can be viewed in the online issue, which is available at wileyonlinelibrary.com.]

The structures of C_2Be_4 cores in the nano-size molecules

The C_2Be_4 double ptC cores maintains in the molecular chains (Fig. 4), planar sheets (Fig. 5), and the thermodynamically favorable tube **TTBB-T18** (Fig. 6). The C—C bond lengths ranging from 1.325 to 1.348 Å are slightly shorter than the C—C bond length (1.351 Å) in free **2a**. The C—Be_T/C—Be_B bond lengths in the assemblies (ranging from 1.610/1.713 to 1.628/1.748 Å, respectively) deviate slightly from that in **2a** unit (1.616/1.720). To characterize the bonding in the nano-size molecules, we performed the B3LYP/6-31G(d) NBO analyses on the representatives (i.e., **TT-C3** chain, **TTBB-P9** sheet, and **TTBB-T18** tube) and the results are included in Table 1. The natural charges on the C, Be_B, and Be_T in these three types of assemblies are in the range of −0.79 approximately −1.09, 0.54–0.85, and 0.65–1.00 |e|, respectively, compared with the values of **2a,** being −1.05, 0.77, and 0.98|e|, respectively, indicating that the part of ionic interactions in C_2Be_4 cores in these assemblies do not change much from those in the isolated **2a.** The total Wiberg bond indices of C—C/C—Be_B/C—Be_T in these assemblies are in the range of 1.83–1.89/0.74–0.87/0.56–0.79, respectively, which are comparable to the values 1.87/0.82/0.60, respectively in the free **2a,** suggesting that the part of covalent bonding interactions in the nano-size molecules do not change obviously from that in the isolated **2a** unit. Overall, the NBO analysis results indicate the nature of chemical bonding of ptC C_2Be_4 core does not change when **2a** units are assembled into nano-size molecules.

The changes in the HOMO–lowest unoccupied molecular orbital (LUMO) gaps

The formations of HBBs in **TT**, **TB**, and **BB** have different effects on the HOMO–LUMO gap. As shown in Table 2, the HOMO–LUMO gaps of **TT** chains are almost identical, being in the range of 3.53–3.50 eV, while those of **TB/BB** chains gradually decrease when the chains becomes longer (decreasing from 3.13/3.30 to 2.93/3.02 eV, respectively). This trend maintains for planar sheets. When the **TTBB** sheets are extended along the direction to form **BB** HBB, the HOMO–LUMO gaps decrease, for example, the HOMO–LUMO gaps for **TTBB-P4**, **TTBB-P9**, and **TTBB-P16** being 3.33, 3.20, and 3.11 eV, respectively. In contrast, if the **TTBB** planar sheets are extended along the direction forming **TT** HBBs, the HOMO–LUMO gaps almost do not change. For example, the gaps for **TTBB-P9**, **TTBB-P15**, and **TTBB-P18** are 3.20, 3.18, and 3.18 eV, respectively. All the HBBs in the **TB** planar sheets are **TB**-type HBBs, thus, extending the **TB** planar sheet along both directions will decrease the HOMO–LUMO gaps. Rolling the planar sheets to nanotubes affect the gaps slightly. For example, the gap (3.14 eV) of the tubular **TTBB-T18** is only 0.04 eV away from that (3.18 eV) from the planar **TTBB-P18.**

Conclusions

In this study, we computationally found a new species (D_{2h} $C_2(BeH)_4$, **2a**) featuring two planar tetracoordinate carbons (ptCs) with electronic structures similar to those of our

previously reported D_{2h} C_2Al_4 (**1**). Aromaticity and the peripheral BeBeBeBe bonding are attributed to the stabilization of the ptC species. We speculate that, although **2a** is not a global minimum, its distinct character of having a C_2 core from that of having separated carbon atoms in global minimum and other low-lying minima could makes **2a** accessible if the carbon source is dominated by C_2 species. In addition, the BOMD simulations demonstrate the good kinetic stability of **2a**. On the basis of the electron deficient Be—H bonds in D_{2h} $C_2(BeH)_4$, we further designed various large/nanostructures including chains, sheets, and tubes utilizing the HBBs. The formations of these large molecules are all highly exothermic, thus, they are potentially realized experimentally. Overall, the geometric and electronic structures of the **2a** units in these nano-size molecules are similar to that of the isolated **2a**.

Keywords: carbon-based planar sheet · thermodynamic stability · planar tetracoordinate carbon · molecular materials · DFT calculations

How to cite this article: X.-F. Zhao, H. Li, C.-X. Yuan, Y.-Q. Li, Y.-B. Wu, Z.-X. Wang. *J. Comput. Chem.* **2016**, *37*, 261–269. DOI: 10.1002/jcc.24018

Additional Supporting Information may be found in the online version of this article.

[1] H. J. Monkhorst, *Chem. Commun. (London)* **1968**, *4*, 1111.
[2] R. Hoffmann, R. W. Alder, C. F. Wilcox, *J. Am. Chem. Soc.* **1970**, *92*, 4992.
[3] J. B. Collins, J. D. Dill, E. D. Jemmis, Y. Apeloig, P. v. R. Schleyer, R. Seeger, J. A. Pople, *J. Am. Chem. Soc.* **1976**, *98*, 5419.
[4] K. Sorger, P. v. R. Schleyer, *J. Mol. Struct. THEOCHEM* **1995**, *338*, 317.
[5] D. Rottger, G. Erker, *Angew. Chem. Int. Ed. Engl.* **1997**, *36*, 813.
[6] L. Radom, D. R. Rasmussen, *Pure Appl. Chem.* **1998**, *70*, 1977.
[7] W. Siebert, A. Gunale, *Chem. Soc. Rev.* **1999**, *28*, 367.
[8] R. Keese, *Chem. Rev.* **2006**, *106*, 4787.
[9] G. Merino, M. A. Mendez-Rojas, A. Vela, T. Heine, *J. Comput. Chem.* **2007**, *28*, 362.
[10] Z. X. Wang, P. v. R. Schleyer, *Science* **2001**, *292*, 2465.
[11] K. Exner, P. v. R. Schleyer, *Science* **2000**, *290*, 1937.
[12] Y. B. Wu, Y. Duan, G. Lu, H. G. Lu, P. Yang, P. v. R. Schleyer, G. Merino, R. Islas, Z. X. Wang, *Phys. Chem. Chem. Phys.* **2012**, *14*, 14760.
[13] A. C. Castro, G. Martinez-Guajardo, T. Johnson, J. M. Ugalde, Y. B. Wu, J. M. Mercero, T. Heine, K. J. Donald, G. Merino, *Phys. Chem. Chem. Phys.* **2012**, *14*, 14764.
[14] C. Crigger, B. K. Wittmaack, M. Tawfik, G. Merino, K. J. Donald, *Phys. Chem. Chem. Phys.* **2012**, *14*, 14775.
[15] J. O. C. Jimenez-Halla, Y. B. Wu, Z. X. Wang, R. Islas, T. Heine, G. Merino, *Chem. Commun.* **2010**, *46*, 8776.
[16] G. A. Rafael, L. C. Jose, I. Rafael, I. Ivan M. M. Jose, R. Alberiro, M. Gabriel, *Phys. Chem. Chem. Phys.* **2015**, *14*, 14760.
[17] P. v. R. Schleyer, A. I. Boldyrev, *J. Chem. Soc. Chem. Commun.* **1991**, *27*, 1536.
[18] S. D. Li, G. M. Ren, C. Q. Miao, Z. H. Jin, *Angew. Chem. Int. Ed.* **2004**, *43*, 1371.
[19] S. D. Li, C. Q. Miao, *J. Phys. Chem. A* **2005**, *109*, 7594.
[20] R. Islas, T. Heine, K. Ito, P. v. R. Schleyer, G. Merino, *J. Am. Chem. Soc.* **2007**, *129*, 14767.
[21] K. Ito, Z. Pu, Q. S. Li, P. v. R. Schleyer, *Inorg. Chem.* **2008**, *47*, 10906.
[22] Z. F. Pu, K. Ito, P. v. R. Schleyer, Q. S. Li, *Inorg. Chem.* **2009**, *48*, 10679.
[23] C. Romanescu, T. R. Galeev, W. L. Li, A. I. Boldyrev, L. S. Wang, *Angew. Chem. Int. Ed.* **2011**, *50*, 9334.
[24] T. Heine, G. Merino, *Angew. Chem. Int. Ed.* **2012**, *51*, 4275.
[25] J. Xu, Y. H. Ding, *J. Comput. Chem.* **2015**, *36*, 355.
[26] C. Romanescu, T. R. Galeev, W. L. Li, A. I. Boldyrev, L. S. Wang, *Acc. Chem. Res.* **2013**, *46*, 350.
[27] X. Li, H. F. Zhang, L. S. Wang, G. D. Geske, A. I. Boldyrev, *Angew. Chem. Int. Ed.* **2000**, *39*, 3630
[28] G. D. Geske, A. I. Boldyrev, *Inorg. Chem.* **2002**, *41*, 2795.
[29] M. Gabriel, A. Miguel, Mendez-Rojas, V. Alberto, *J. Am. Chem. Soc.* **2003**, *125*, 6026.
[30] P. D. Pancharatna, M. A. Mendez-Rojas, G. Merino, A. Vela, R. Hoffmann, *J. Am. Chem. Soc.* **2004**, *126*, 15309.
[31] L. M. Yang, Y. H. Ding, C. C. Sun, *J. Am. Chem. Soc.* **2007**, *129*, 658.
[32] L. M. Yang, Y. H. Ding, W. Q. Tian, C. C. Sun, *Phys. Chem. Chem. Phys.* **2007**, *9*, 5304.
[33] L. M. Yang, Y. H. Ding, C. C. Sun, *Theor. Chem. Acc.* **2008**, *119*, 335.
[34] L. M. Yang, H. P. He, Y. H. Ding, C. C. Sun, *Organometallics* **2008**, *27*, 1727.
[35] L. M. Yang, X. P. Li, Y. H. Ding, C. C. Sun, *J. Mol. Model.* **2009**, *15*, 97.
[36] X. J. Wu, Y. Pei, X. C. Zeng, *Nano Lett.* **2009**, *9*, 1577.
[37] X. Y. Luo, J. H. Yang, H. Y. Liu, X. J. Wu, Y. C. Wang, Y. M. Ma, S. H. Wei, X. G. Gong, H. J. Xiang, *J. Am. Chem. Soc.* **2011**, *133*, 16285.
[38] M. H. Wu, Y. Pei, X. C. Zeng, *J. Am. Chem. Soc.* **2010**, *132*, 5554.
[39] B. Xiao, Y. H. Ding, C. C. Sun, *Phys. Chem. Chem. Phys.* **2011**, *13*, 2732.
[40] M. H. Wu, Y. Pei, J. Dai, H. Li, X. C. Zeng, *J. Phys. Chem. C* **2012**, *116*, 11378.
[41] M. H. Wu, Y. Pei, X. C. Zeng, *Chem. Phys. Lett.* **2013**, *580*, 78.
[42] Y. F. Li, Y. L. Liao, P. v. R. Schleyer, Z. F. Chen, *Nanoscale* **2014**, *6*, 10784.
[43] J. Dai, X. J. Wu, J. L. Yang, X. C. Zeng, *J. Phys. Chem. Lett.* **2014**, *5*, 2058.
[44] Z. H. Zhang, X. F. Liu, B. I. Yakobson, W. L. Guo, *J. Am. Chem. Soc.* **2012**, *134*, 19326.
[45] Y. F. Li, Y. L. Liao, Z. F. Chen, *Angew. Chem. Int. Ed.* **2014**, *53*, 7248.
[46] A. Nandula, Q. T. Trinh, M. Saeys, A. N. Alexandrova, *Angew. Chem. Int. Ed.* **2015**, *54*, 5312.
[47] L. M. Yang, V. Bacic, I. A. Popov, A. I. Boldyrev, T. Heine, T. Frauenheim, E. Ganz, *J. Am. Chem. Soc.* **2015**, *137*, 2757.
[48] Y. F. Li, F. Y. Li, Z. Zhou, Z. F. Chen, *J. Am. Chem. Soc.* **2011**, *133*, 900.
[49] B. Xiao, X. F. Yu, H. Hu, Y. H. Ding, *Chem. Phys. Lett.* **2014**, *608*, 277.
[50] Y. B. Wu, C. X. Yuan, F. Gao, H. G. Lu, J. C. Guo, S. D. Li, Y. K. Wang, P. Yang, *Organometallics* **2007**, *26*, 4395.
[51] W. X. Sun, C. J. Zhang, Z. X. Cao, *J. Phys. Chem. C* **2008**, *112*, 351.
[52] C. J. Zhang, W. X. Sun, Z. X. Cao, *J. Am. Chem. Soc.* **2008**, *130*, 5638.
[53] Y. B. Wu, Z. X. Li, X. H. Pu, Z. X. Wang, *J. Phys. Chem. C* **2011**, *115*, 13187.
[54] Y. B. Wu, Z. X. Li, X. H. Pu, Z. X. Wang, Comput. *Theor. Chem.* **2012**, *992*, 78.
[55] Y. B. Wu, J. L. Jiang, H. Li, Z. F. Chen, Z. X. Wang, *Phys. Chem. Chem. Phys.* **2010**, *12*, 58.
[56] Y. B. Wu, J. L. Jiang, R. W. Zhang, Z. X. Wang, *Chem. Eur. J.* **2010**, *16*, 1271.
[57] M. Saunders, *J. Comput. Chem.* **2004**, *25*, 621.
[58] P. P. Bera, K. W. Sattelmeyer, M. Saunders, H. F. Schaefer, P. v. R. Schleyer, *J. Phys. Chem. A* **2006**, *110*, 4287.
[59] A. E. Reed, L. A. Curtiss, F. Weinhold, *Chem. Rev.* **1988**, *88*, 899.
[60] P. v. R. Schleyer, C. Maerker, A. Dransfeld, H. J. Jiao, N. Hommes, *J. Am. Chem. Soc.* **1996**, *118*, 6317.
[61] Z. F. Chen, C. S. Wannere, C. Corminboeuf, R. Puchta, P. v. R. Schleyer, *Chem. Rev.* **2005**, *105*, 3842.
[62] J. R. Cheeseman, G. W. Trucks, T. A. Keith, M. J. Frisch, *J. Chem. Phys.* **1996**, *104*, 5497.
[63] J. M. Millam, V. Bakken, W. Chen, W. L. Hase, H. B. Schlegel, *J. Chem. Phys.* **1999**, *111*, 3800.
[64] H. G. Lu, Y. B. Wu, GXYZ, A Random Cartesian Coordinates Generating Program; Shanxi University: Taiyuan, China, **2008**.
[65] M. J. Frisch, G. W. Trucks, H. B. Schlegel, G. E. Scuseria, M. A. Robb, J. R. Cheeseman, G. Scalmani, V. Barone, B. Mennucci, G. A. Petersson, H. Nakatsuji, M. Caricato, X. Li, H. P. Hratchian, A. F. Izmaylov, J. Bloino, G. Zheng, J. L. Sonnenberg, M. Hada, M. Ehara, K. Toyota, R. Fukuda, J. Hasegawa, M. Ishida, T. Nakajima, Y. Honda, O. Kitao, H. Nakai, T. Vreven, J. A. Montgomery, J. E. Peralta, F. Ogliaro, M. Bearpark, J. J. Heyd, E. Brothers, K. N. Kudin, V. N. Staroverov, T. Keith, R. Kobayashi, J.

Normand, K. Raghavachari, A. Rendell, J. C. Burant, S. S. Iyengar, J. Tomasi, M. Cossi, N. Rega, J. M. Millam, M. Klene, J. E. Knox, J. B. Cross, V. Bakken, C. Adamo, J. Jaramillo, R. Gomperts, R. E. Stratmann, O. Yazyev, A. J. Austin, R. Cammi, C. Pomelli, J. W. Ochterski, R. L. Martin, K. Morokuma, V. G. Zakrzewski, G. A. Voth, P. Salvador, J. J. Dannenberg, S. Dapprich, A. D. Daniels, O. Farkas, J. B. Foresman, J. V. Ortiz, J. Cioslowski, D. J. Fox, Gaussian 09 Revision D.01; Gaussian: Wallingford, CT, **2013**.

[66] H.-J. Werner, P. J. Knowles, G. Knizia, F. R. Manby, M. Schütz, P. Celani, T. Korona, R. Lindh, A. Mitrushenkov, G. Rauhut, K. R. Shamasundar, T. B. Adler, R. D. Amos, A. Bernhardsson, A. Berning, D. L. Cooper, M. J. O. Deegan, A. J. Dobbyn, F. Eckert, E. Goll, C. Hampel, A. Hesselmann, G. Hetzer, T. Hrenar, G. Jansen, C. Köppl, Y. Liu, A. W. Lloyd, R. A. Mata, A. J. May, S. J. McNicholas, W. Meyer, M. E. Mura, A. Nicklass, D. P. O'Neill, P. Palmieri, D. Peng, K. Pflüger, R. Pitzer, M. Reiher, T. Shiozaki, H. Stoll, A. J. Stone, R. Tarroni, T. Thorsteinsson, M. Wang, MolPro 2012.1; University College Cardiff Consultants Limited: Cardiff, U.K., **2012**.

[67] Y. B. Wu, H. G. Lu, S. D. Li, Z. X. Wang, *J. Phys. Chem. A* **2009**, *113*, 3395.

[68] Z. X. Wang, P. v. R. Schleyer, *J. Am. Chem. Soc.* **2001**, *123*, 994.

[69] Y. Pei, W. An, K. Ito, P. v. R. Schleyer, X. C. Zeng, *J. Am. Chem. Soc.* **2008**, *130*, 10394.

Received: 27 March 2015
Revised: 27 June 2015
Accepted: 30 June 2015
Published online on 22 July 2015